Effect of Light on Self-Assembly of Aqueous Mixtures of Sodium Dodecyl Sulfate and a Cationic, Bolaform Surfactant Containing Azobenzene

F. Pierce Hubbard, Jr., and Nicholas L. Abbott*

Department of Chemical and Biological Engineering, University of Madison−Wisconsin, 1415 Engineering Drive, Madison, Wisconsin 53706-1691

Received November 2, 2006. In Final Form: January 9, 2007

We report light and small-angle neutron scattering measurements that characterize microstructures formed in aqueous surfactant solutions (up to 1.0 wt % surfactant) containing mixtures of sodium dodecyl sulfate (SDS) and the light-sensitive bolaform surfactant, bis(trimethylammoniumhexyloxy)azobenzene dibromide (BTHA) as a function of composition, equilibration time, and photostationary state (i.e., solutions rich in *cis*-BTHA or *trans*-BTHA). We observed formation of vesicles in both SDS-rich and *trans*-BTHA-rich regions of the microstructure diagram, with vesicles present over a particularly broad range of compositions for *trans*-BTHA-rich solutions. Illumination of mixtures of BTHA and SDS with a broadband UV light source leads to formation of photostationary states where the fraction of BTHA present as cis isomer (75−80% *cis*-BTHA) is largely independent of the mixing ratio of SDS and BTHA. For a relatively limited set of mixing ratios of SDS and BTHA, we observed UV illumination of SDS-rich vesicles to result in the reversible transformation of the vesicles to micellar aggregates and UV illumination of BTHA-rich vesicles to result in irreversible precipitation. Surprisingly, however, for many mixtures of *trans*-BTHA and SDS that formed solutions containing vesicles, illumination with UV light (which was confirmed to lead to photoisomerization of BTHA) resulted in only a small decrease in the number of vesicles in solution, relatively little change in the sizes of the remaining vesicles, and coexistance of the vesicles with micelles. These observations are consistent with a physical model in which the trans and cis isomers of BTHA present at the photostationary state tend to segregate between the different microstructures coexisting in solution (e.g., vesicles rich in *trans*-BTHA and SDS coexist with micelles rich in *cis*-BTHA and SDS). The results presented in this paper provide guidance for the design of light-tunable surfactants systems.

Introduction

The self-assembly of surfactants into microstructures such as globular micelles, wormlike micelles, or vesicles provides a means to engineer a wide range of solution properties.[1−3] The development of principles that permit conversion of one type of microstructure to another through control of an easily adjusted external variable would therefore enable the development of methods to actively tune such solution properties. Toward this end, recent studies have demonstrated that changes in aggregate microstructure can be triggered by illumination of solutions containing light-sensitive surfactants. For example, vesicle-to-micelle transitions,[4,5] and vesicle-to-lamellae transitions[6] have been reported for aqueous solutions of light-sensitive surfactants. The majority of reports on light-sensitive surfactant systems make use of the azobenzene group,[5−22] although other moieties such as stilbenes[4,23−25] and spriopyrans[26,27] have also been used. Azobenzene is an attractive photosensitive group because of its robust and simple photochemistry and because of the ease with which it can be incorporated into various types of surfactant architectures.

In this paper, we report on the phase behavior and microstructure of aqueous mixtures of sodium dodecyl sulfate (SDS) and a bolaform, cationic, light-sensitive surfactant, bis(trim-

* Corresponding author. E-mail: abbott@engr.wisc.edu. Phone: +1-608-265-5278. Fax: +1-608-262-5434.

(1) Cates, M. E.; Candau, S. J. *J. Phys.: Condens. Matter* **1990**, *2*, 6869−6892.
(2) Walde, P. *Perspect. Supramol. Chem.* **2000**, *6*, 297−311.
(3) Kano, K.; Romero, A.; Djermouni, B.; Ache, H. J.; Fendler, J. H. *J. Am. Chem. Soc.* **1979**, *101*, 4030−4037.
(4) Eastoe, J.; Dominguez, M. S.; Wyatt, P.; Heenan, R. K. *Langmuir* **2004**, *20*, 6120−6126.
(5) Hubbard, Jr., F. P.; Santonicola, G.; Kaler, E. W.; Abbott, N. L. *Langmuir* **2005**, *21*, 6131−6136.
(6) Sakai, H.; Matsumura, A.; Yokoyama, S.; Saji, T.; Abe, M. *J. Phys. Chem. B* **1999**, *103*, 10737−10740.
(7) Shin, J. Y.; Abbott, N. L. *Langmuir* **1999**, *15*, 4404−4410.
(8) Kang, H.-C.; Lee, B. M.; Yoon, J.; Yoon, M. *J. Colloid Interface Sci.* **2000**, *231*, 255−264.
(9) Orihara, Y.; Matsumura, A.; Saito, Y.; Ogawa, N.; Saji, T.; Yamaguchi, A.; Sakai, H.; Abe, K. *Langmuir* **2001**, *17*, 6072−6076.
(10) Buwalda, R. T.; Stuart, M. C. A.; Engberts, J. B. F. N. *Langmuir* **2002**, *18*, 6507−6512.
(11) Zou, B.; Qiu, D.; Hou, X.; Wu, L.; Zhang, X.; Chi, L.; Fuchs, H. *Langmuir* **2002**, *18*, 8006−8009.
(12) Eastoe, J.; Dominguez, M. S.; Cumber, H.; Burnett, G.; Wyatt, P.; Heenan, R. K. *Langmuir* **2003**, *19*, 6579−6581.
(13) Shang, T.; Smith, K. A.; Hatton, T. A. *Langmuir* **2003**, *19*, 10764−10773.
(14) Eastoe, J.; Dominguez, M. S.; Cumber, H.; Wyatt, P.; Heenan, R. K. *Langmuir* **2004**, *20*, 1120−1125.
(15) Lee, C. T.; Smith, K. A.; Hatton, T. A. *Macromolecules* **2004**, *37*, 5397−5405.
(16) Bonini, M.; Berti, D.; Di, Meglio, J. M.; Almgren, M.; Teixeria, J.; Baglioni, P. *Soft Matter* **2005**, *1*, 444−454.
(17) Faure, D.; Gravier, J.; Labrot, T.; Desbat, B.; Oda, R.; Bassani, D. M. *Chem. Commun.* **2005**, *9*, 1167−1169.
(18) Lee, C. T.; Smith, K. A.; Hatton, T. A. *Biochemistry* **2005**, *44*, 524−536.
(19) Sakai, H.; Orihara, Y.; Kodashima, H.; Matsumura, A.; Ohkubo, T.; Tsuchiya, K.; Abe, M. *J. Am. Chem. Soc.* **2005**, *127*, 13454−13455.
(20) Bradley, M.; Vincent, B.; Warren, N. *Langmuir* **2006**, *22*, 101−105.
(21) Eastoe, J.; Vesperinas, A.; Donnewirth, A.-C.; Wyatt, P.; Grillo, I.; Heenan, R. K.; Davis, S. *Langmuir* **2006**, *22*, 851−853.
(22) Shang, T.; Smith, K. A.; Hatton, T. A. *Langmuir* **2006**, *22*, 1436−1442.
(23) Kozlecki, T.; Wilk, K. A. *J. Phys. Org. Chem.* **1996**, *9*, 645−651.
(24) Kozlecki, T.; Wilk, K. A.; Syper, L. *Prog. Colloid Polym. Sci.* **1998**, *110*, 193−198.
(25) Eastoe, J.; Dominguez, M. S.; Wyatt, P.; Beeby, A.; Heenan, R. K. *Langmuir* **2002**, *18*, 7837−7844.
(26) Liu, S.; Fujihira, M.; Saji, T. *J. Chem. Soc., Chem. Commun.* **1994**, *16*, 1855−1856.
(27) Sun, C.; Arimitsu, K.; Abe, K.; Ohkubo, T.; Yamashita, T.; Sakai, H.; Abe, M. *Mater. Technol.* **2004**, *22*, 229−237.

10.1021/la0632124 CCC: $37.00
Published on Web 03/24/2007

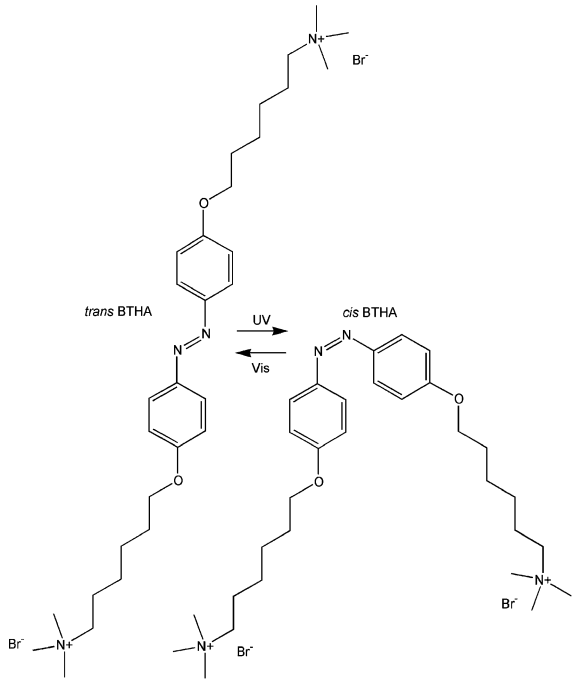

Figure 1. Molecular structures of the trans and cis isomers of BTHA.

ethylammoniumhexyloxy)azobenzene dibromide (BTHA). As depicted in Figure 1, illumination of the azobenzene moiety with ultraviolet light drives a trans to cis isomerization of BTHA. The reverse process can be driven by illumination of a cis isomer of BTHA with visible light or can occur thermally by allowing a solution rich in the cis isomer of BTHA to equilibrate in the dark for a period of hours. Our study builds from a prior investigation in which we reported that aqueous solutions containing mixtures of SDS and BTHA undergo substantial reorganization upon illumination[7,28] and, in particular, that solutions containing 0.1 wt % total surfactant and a molar ratio of SDS to BTHA of ~5.6 displayed a reversible vesicle-to-micelle transition upon illumination with light.[5] A subsequent publication by Bonini et al. confirmed the latter conclusion using a solution containing a SDS to BTHA ratio of 4.8.[16] The study reported here goes beyond these past papers by investigating the phase behavior and microstructures formed in solutions of BTHA and SDS that contain a broader range of compositions than previously studied (0.1−1.0 wt % total surfactant and between 5 and 90 mol % BTHA). We report characterization of the aqueous surfactant solutions before and after illumination with UV light in order to understand the impact of photoisomerization of BTHA on the phase behavior and microstructure of the solutions containing various mixtures. The overall goal of the study was to provide a more comprehensive description of the properties of this light-sensitive surfactant system.

A range of experimental techniques have been used to characterize phase behavior and microstructure of mixed surfactant systems, including visual inspection, quasi-elastic light scattering (QLS), small-angle neutron scattering (SANS), and cryo-electron microscopy (cryo-TEM).[6,29,30] Visual inspection of a sample can reveal whether it contains more than one phase, whether precipitate is formed, and whether the solution is turbid or not. Past studies have also concluded that the presence of vesicles typically results in solutions with a slight bluish hue.[29] Quasi-elastic light scattering measurements are commonly used to estimate the hydrodynamic diameters of aggregates present in solution. These measurements cannot, however, reveal information about the shape of the aggregates and are difficult to interpret when the solutions contain a mixture of aggregates. To obtain information about aggregate shape, cryo-TEM or SANS is commonly used.[6,29] In this work, we have combined visual observations with QLS and SANS experiments to characterize the microstructures formed in solution by SDS and BTHA.

The results presented in this paper are organized into three sections. First, we report on the phase behavior and microstructure of aqueous solutions containing *trans*-BTHA and SDS after various periods of equilibration. Second, we describe the results of a study of the photoisomerization of these surfactant mixtures as a function of composition. Specifically, we sought to determine whether the photostationary state was a function of the composition of SDS and BTHA in solution. Third, we report on the phase behavior and composition of cis-rich BTHA solutions and thus identify the changes in phase behavior and microstructure that can accompany photoisomerization of BTHA in this mixed surfactant system.

Experimental Section

Materials. All reagents were obtained from Aldrich (Milwaukee, WI). SDS was recrystallized three times in ethanol prior to use.[5,7] BTHA was synthesized as previously described and recrystallized three times in ethanol prior to use.[5,7] D_2O (99.9% deuteration) was obtained from Cambridge Isotope Laboratories (Andover, MA).

Methods. Stock solutions of either BTHA or SDS were prepared by weighing the appropriate mass of surfactant into a scintillation vial and then adding deionized and distilled H_2O (18.2 MΩ cm, Millipore, Billerica, MA) or D_2O. Surfactant mixtures were prepared by mixing stock solutions filtered through a 0.22-μm Millex-GV filter. For QLS measurements, surfactant mixtures were prepared in 12-mm-diameter borosilicate test tubes (Fisher, Atlanta, GA) that were cleaned with piranha solution (70% H_2SO_4, 30% H_2O_2) prior to use. *WARNING: Piranha solution should be handled with extreme caution; in some circumstances (most probably when it has been mixed with significant quantities of an oxidizable organic material), it has detonated unexpectedly.* The test tubes were sealed with polyethylene caps (Andwin Scientific, Addison, IL). Prior to use, the caps were soaked in a SDS solution overnight, rinsed thoroughly with water and ethanol, and dried under vacuum. Care was taken to ensure that the surfactant solution to be examined did not come into contact with the caps. After sealing, samples were placed in a circulating water bath, which was maintained at 25 °C. The bath was covered with aluminum foil to prevent exposure of the samples to light. Samples were visually inspected after various periods of time using ambient light and then returned to the water bath. For SANS measurements, solutions were prepared in small scintillation vials and sealed with Teflon screw caps prior to measurement.

UV−Vis Measurements. Because the molar absorptivity of BTHA is high ($\epsilon = 2320$ m^2/mol at 360 nm), samples were diluted to a final concentration of 30 μM BTHA prior to UV−vis measurement. Optical absorption spectra were recorded using a Cary 1E UV−vis spectrophotometer (Varian, Walnut Creek, CA). For *trans*-BTHA, samples were equilibrated in the dark overnight and then diluted prior to measurement. *cis*-BTHA samples were illuminated with ultraviolet (UV) light and then diluted prior to measurement. Similarly, samples subjected to a photocycle (trans to cis to trans) were illuminated with UV and then visible light, and the resulting solution was diluted prior to measurement. The absorbance peak for a solution of *trans*-BTHA (no SDS) occurs at 360 nm. By comparing the absorbance of the solutions at 360 nm, we determined that typical trans-to-cis conversions using UV light

(28) Shin, J. Y.; Abbott, N. L. In *Mixed Surfactant Systems*, 2nd ed.; Abe, M., Scamehorn, J. F., Eds.; Marcel Dekker: New York, 2005; Vol. 124.
(29) Yatcilla, M.; Herrington, K.; Brasher, L.; Kaler, E. *J. Phys. Chem.* **1996**, *100*, 5874−5879.
(30) Brasher, L.; Kaler, E. *Langmuir* **1996**, *12*, 6270−6276.

led to solutions containing 75−80% of the cis isomer. Conversions of *cis*-BTHA to *trans*-BTHA using visible light were found to be nearly complete, resulting in solutions composed of 90%+ trans isomer.

Photoisomerization Protocol. *trans*-BTHA solutions were illuminated using a Spectroline E-Series lamp with filter (model EN280L, Westbury, NY) to produce a solution enriched with the cis isomer. The lamp emitted UV light with wavelengths from 300 to 450 nm, with peak intensity at 365 nm. The filter was designed to eliminate light with wavelengths greater than 410 nm. *cis*-BTHA solutions were illuminated with an ordinary desk lamp fitted with a 100-W incandescent bulb to create solutions rich in the trans isomer.

Solutions containing 0.3 wt % total surfactant or less were illuminated in 12-mm-diameter borosilicate test tubes. Illumination for 30 min was sufficient to reach the photostationary state. Solutions with greater than 0.3 wt % total surfactant were passed through a home-built flow cell for isomerization. The flow cell was composed of two glass microscope slides (Fisher, Atlanta, GA) separated by a 100-μm plastic spacer cemented together using GE RTV118 silicone cement (MG Chemicals, Surrey, British Columbia). Two $^1/_8$-in holes were drilled in the top slide, to which two plastic ports were cemented. Solutions to be illuminated were drawn into a length of silicone tubing (Cole Parmer FF-95802-03, Vernon Hills, IL) using a 3-mL plastic syringe (BD, Franklin Lakes, NJ). The tubing was soaked in a SDS solution overnight and then flushed with water prior to use. The tubing containing solution was connected to one flow cell port and passed through the flow cell at a controlled rate using a KDS230 syringe pump (KD Scientific, Holliston, MA). The solution exiting the flow cell was collected in a test tube. Prior to QLS and SANS measurements, the flow rate necessary to reach the photostationary state was determined for each sample and was identified as the point where the UV−vis spectra of the solution did not change with further illumination. Typical flow rates ranged from 1.5 to 2.0 mL/h (corresponding to a residence time within the flow cells of ∼4 min), depending on the total surfactant concentration.

The cis isomer of BTHA is not persistent in solution; *cis*-BTHA will relax back to *trans*-BTHA if left in the dark over a period of hours.[5,7] Thus, for QLS and SANS measurements, we chose to characterize solutions rich in the cis isomer of BTHA under continuous illumination with UV light after the photostationary state had been reached, to avoid complexities introduced by these relaxation dynamics.

Quasi-Elastic Light Scattering. Quasi-elastic light scattering measurements were conducted using a Brookhaven light scattering apparatus (Brookhaven Instruments, Holtsville, NY), composed of a BI-9000AT digital autocorrelator, a BI-200SM goniometer, and a 25-mW laser (637 nm, Coherent Radius 635-25). The detector angle was set to 90°, and the autocorrelation curves were analyzed using the method of cumulants.[31] This method provides the average decay rate, $\langle\tau\rangle = \langle D_T\rangle q^2$, where $\langle D_T\rangle$ is the average translational diffusion coefficient and q is the magnitude of the scattering vector. The normalized, relative variance is calculated as, $\nu = (\langle\tau^2\rangle - \langle\tau\rangle^2)/\langle\tau\rangle^2$. $\langle D_T\rangle$ is related to the hydrodynamic diameter according to the Stokes−Einstein equation.[32] Measurements at other angles (50°−130°) confirmed that the autocorrelation functions recorded corresponded to center of mass diffusion of the aggregates in solution.

Small-Angle Neutron Scattering. Small-angle neutron scattering measurements were performed using the NG3 instrument at National Institute of Standards and Technology (NIST) in Gaithersburg, MD. The wavelengths of the neutrons were on average 6 Å, with a spread in wavelength, $\Delta\lambda/\lambda$, of 14%. Data were collected with the detector set at two positions: 1.9 and 13.17 m from the sample. By offsetting the detector 25 cm from center, these distances covered q-ranges of 0.02−0.35 and 0.0035−0.05 Å^{-1}, res pectively, where q is the magnitude of the scattering vector. Samples were held in quartz cells with a path length of 2.0 mm and placed in a sample chamber thermostated at 25.0 ± 0.1 °C. To ensure good statistics, at least 10^6 detector counts were collected for each sample at each distance. The data were corrected for detector efficiency, background radiation, empty cell scattering, and incoherent scattering to calculate the scattered intensity on an absolute scale. These procedures were performed using a computer program provided by NIST that runs on IGOR Pro (Wavemetrics, Lake Owego, OR).

We used Guinier analysis and form factor modeling to interpret SANS spectra. Both of these techniques have been discussed extensively in the literature[5,30,33−36] and are only summarized here. The scattered intensity, $I(q)$, is related to the differential scattering cross section, $d\Sigma(q)/d\Omega$, by

$$I(q) = \int R(q)\frac{d\Sigma(q)}{d\Omega}\,dq \tag{1}$$

where $R(q)$ is the resolution function, accounting for instrumental smearing effects such as wavelength spread, imperfect collimation, and finite slit width/length effects.

The differential scattering cross section can be expressed in terms of a form factor, $P(q)$, and a structure factor, $S(q)$. For samples identified by Guinier analysis to contain vesicles, we used a polydisperse core−shell model for $P(q)$, in which the vesicles have a polydisperse core radius and a constant shell thickness. Because the vesicle solutions characterized in our study were dilute (the spacing between vesicles is more than twice the average vesicle diameter), we set $S(q) = 1$ in our analysis of these solutions. The good agreement between the calculated and measured scattered intensity (see below) provides further justification for this assumption. The differential scattering cross section was thus evaluated as[36]

$$\frac{d\Sigma(q)}{d\Omega} = n\int_0^\infty G(r_c)P^2(qr_c)\,dr_c \tag{2}$$

where n is the number density of vesicles, r_c is the core radius, $G(r_c)$ is the distribution of core radii, and $P^2(qr_c)$ is the form factor for a single vesicle. The distribution of vesicle sizes was modeled as a Schultz distribution,[5,36]

$$G(r_c) = \frac{r_c^{\,Z}}{\Gamma(Z+1)}\left(\frac{Z+1}{\bar{r}_c}\right)^{Z+1}\exp\left(\frac{-r_c}{\bar{r}_c}(Z+1)\right) \tag{3}$$

where Γ is the gamma function, $\bar{r}_c$ is the mean core radius, and Z is related to the variance of the core radii (σ^2) by

$$\frac{1}{Z+1} = \frac{\sigma^2}{\bar{r}_c^{\,2}} \tag{4}$$

The form factor for a single vesicle is

$$P(qr_c) = \frac{4\pi}{q^3}(\rho_v - \rho_s)\{[\sin q(r_c + t) - \sin qr_c] - [q(r_c + t)\cos q(r_c + t) - qr_c\cos qr_c]\} \tag{5}$$

where ρ_v and ρ_s represent the scattering length density of the vesicle and solvent, respectively, and t is the shell thickness. Thus, the fitting parameters of this model are the core radius and polydispersity, the shell thickness, and the volume fraction of aggregates.[30]

Samples identified to contain micelles via Guinier analysis were fit using a monodisperse ellipsoidal form factor combined with a screened Coulomb model for the structure factor. The differential scattering cross section is expressed as

(31) Koppel, D. E. *J. Chem. Phys.* **1972**, *57*, 4814−4820.
(32) Hiemenz, P. C.; Rajagopalan, R. *Principles of Colloid and Surface Chemistry*, 3rd ed.; Marcel Dekker: New York, 1997.
(33) Guinier, A.; Fournet, G. *Small Angle Scattering of X-Rays*; John Wiley & Sons: New York, 1955.
(34) Porod, G. In *Small Angle X-ray Scattering*; Glatter, O., Kratky, O., Eds.; Academic Press, Inc.: London, 1982.
(35) Hassan, P. A.; Fritz, G.; Kaler, E. W. *J. Colloid Interface Sci.* **2003**, *257*, 154−162.
(36) Gonzalez, Y. I.; Stjerndahl, M.; Danino, D.; Kaler, E. W. *Langmuir* **2004**, *20*, 7053−7063.

$$\frac{d\Sigma(q)}{d\Omega} = n_p P(q) S'(q) \quad (6)$$

where n_p is the number density of particles and $S'(q)$ is the structure factor averaged over all possible orientations (necessary for anisotropic particles). The form factor for an ellipsoid of revolution (prolate or oblate) is[37]

$$P(q) = \int_0^1 |F(q,x)|^2 \, dx \quad (7)$$

$$F(q,x) = V_e(\rho_e - \rho_s)\frac{3(\sin z - z\cos z)}{z^3} \quad (8)$$

$$z = qr_b[1 + x^2(\upsilon^2 - 1)]^{1/2}, \quad \upsilon = \frac{r_a}{r_b} \quad (9)$$

where ρ_e and ρ_s are the scattering length densities of the ellipsoid and solvent, V_e is the volume of the ellipsoid $= (4/3)\pi r_a r_b^2$, r_a is the axis of revolution of the ellipsoid, and r_b is the other axis. Thus, when $r_a > r_b$, the model corresponds to prolate ellipsoids, and when $r_a < r_b$, the model corresponds to oblate ellipsoids. We used the rescaled mean spherical approximation procedure developed by Hayter, Hanson, and Penfold combined with the Yukawa form of the potential to evaluate the structure factor, S(q), during our fitting procedure. The interested reader is referred to the original papers for more information.[38,39] The relationship between $S(q)$ and $S'(q)$ is[35,36,40]

$$S'(q) = 1 + \frac{\langle F(q,x)\rangle^2}{\langle |F(q,x)|^2\rangle}(S(q) - 1) \quad (10)$$

In evaluating the structure factor, the ellipsoid is treated as a equivalent rigid sphere with diameter $d = 2(r_a r_b^2)^{1/3}$. Accounting for the polydispersity of the micelles introduces extra parameters into the fit and thus was not done. We calculated parameters in the model as follows. The surfactant molecular volumes, scattering length density,[37] and dielectric constant of water have been reported in past publications.[16] The scattering length density of each surfactant was calculated from the atomic composition. We calculated the scattering length density for an aggregate by assuming a 1:2 ratio of BTHA to SDS in each aggregate. The ionic strength of the solution was estimated based on the amount of free surfactant in solution and the counterions released from the micelles upon addition of BTHA. We estimated the concentration of free counterions by assuming that all of the BTHA is incorporated into the SDS micelles and that each molecule of BTHA that is added results in the release of two Br^- and two Na^+ ions. When analyzing samples containing micelles, the major axis, the minor axis, the micelle surface charge, and the volume fraction of aggregates were used as fitting parameters.

Results and Discussion

1. Phase Behavior and Microstructure of Solutions Containing *trans*-BTHA and SDS. Figure 2 shows the microstructure diagram for *trans*-BTHA/SDS mixtures obtained after 1 day (A) and 6 months (B) of equilibration in the dark at 25 °C. Similar plots at intermediate equilibration times (1 week, 1 month) can be found in Supporting Information. Compositions indicated by (O) correspond to samples characterized by both QLS and SANS, whereas (+) is used to indicate samples investigated with QLS only. Regions of the plots corresponding to different microstructures are separated by solid lines. The solid line from the apex of each diagram to the base indicates a composition of

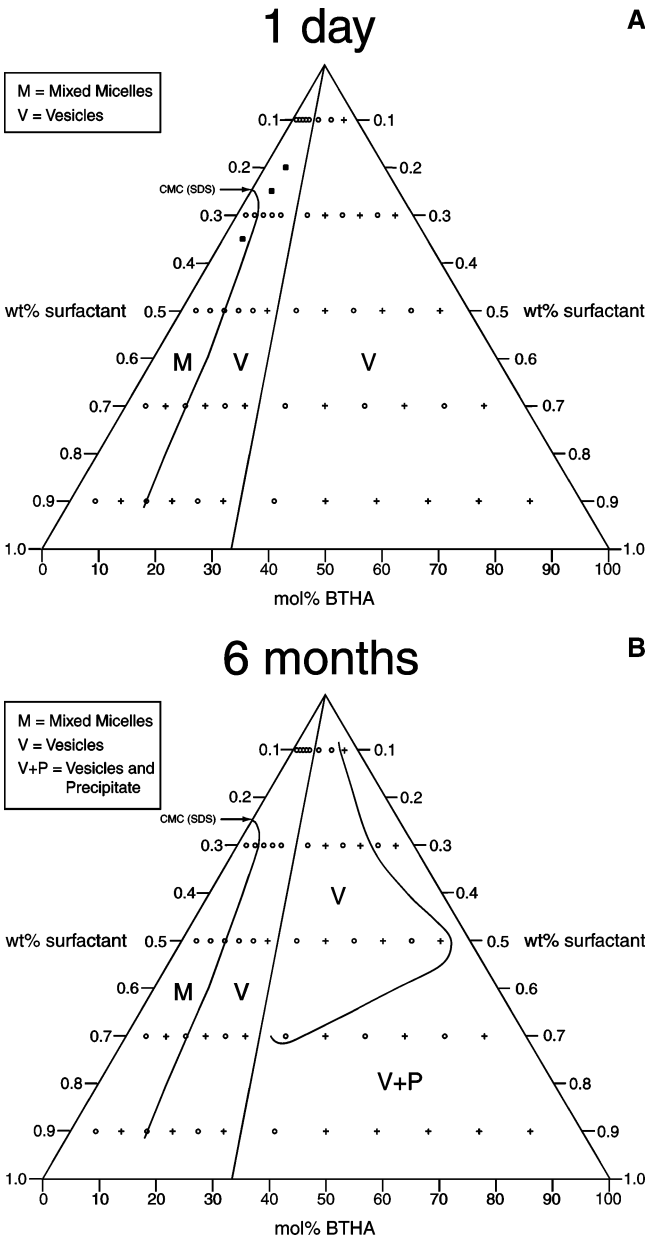

Figure 2. Microstructure diagram for SDS/*trans*-BTHA/H_2O after 1 day (A) and 6 months (B) of equilibration in the dark at 25 °C. The density of points sampled is indicated on the diagram. Samples investigated with both QLS and SANS are marked with a (O), whereas samples investigated only with QLS are marked with a (+). Samples marked with solid squares represent results from a separate work.[16] The solid line drawn from the apex to the base represents solutions that contain an equal number of positively and negatively charged surfactant head groups (33 mol % BTHA), where all samples precipitate.

33 mol % BTHA, where all samples were observed to precipitate. This mixing ratio corresponds to solutions that are charge neutral with respect to the number of surfactant head groups and is comparable to conventional surfactant systems in which the charge neutral point is an equimolar ratio of cationic to anionic surfactant.[29] We note here that we refer to compositions that lie to the left of this line as being SDS-rich, whereas solutions with compositions that lie to the right are described in this paper as being BTHA-rich. Below we discuss in detail our characterization of the microstructures indicated in the various parts of Figure 2. This characterization was based on (i) visual inspection, (ii) light scattering measurements, and (iii) small-angle neutron

(37) Feigin, L. A.; Svergun, D. I. *Structure Analysis by Small-Angle X-Ray and Neutron Scattering*; Plenum Press: New York, 1987.
(38) Hayter, J. B.; Penfold, J. *Mol. Phys.* **1981**, *42*, 109−118.
(39) Hansen, J.-P.; Hayter, J. B. *Mol. Phys.* **1982**, *46*, 651−656.
(40) Sheu, E. Y.; Wu, C. F.; Chen, S. H. *J. Phys. Chem.* **1986**, *90*, 4179−4187.

Table 1. Quasi-Elastic Light Scattering Results and Parameter Estimates Obtained from Form Factor Fits to the SANS Data for the Solutions Containing 0.5 wt % Total Surfactant Presented in Figure 3

sample (mol %)	QLS diameter (nm) H_2O/D_2O	major axis (nm)	minor axis (nm)	charge (e)	$\sqrt{\chi^2/N}$
5	18/13	2.7	1.8	23	1.4
10	18/13	3.2	1.9	20	1.4
100	79/89				

sample (mol %)	QLS diameter (nm) H_2O/D_2O	form factor diameter (nm)	polydis-persity	bilayer thickness (nm)	$\sqrt{\chi^2/N}$
20	122/122	47	0.34	2.6	5.2
25	130/142	47	0.37	2.8	2.3
40	177/235	168	0.30	2.9	2.3
60	197/256	176	0.30	2.9	2.5

scattering. Conclusions reached by use of each technique are described in sequence below.

SDS-Rich Solutions. Prior to QLS and SANS measurements, all samples were visually inspected. Samples identified later to contain micelles were brightly colored, but completely transparent, whereas samples that were determined to contain vesicles were slightly turbid. As indicated in Figure 2, for very dilute concentrations (0.1 wt % total surfactant) of surfactant, vesicles were observed to form in samples that contained 5−90 mol % BTHA. As the total surfactant concentration was increased, we observed that the width of the vesicle region decreased in favor of mixed micelles at high SDS/BTHA ratios. This result is qualitatively similar to that observed for mixtures of cetyltrimethylammonium bromide (CTAB) and sodium octyl sulfate (SOS).[29] Inspection of Figure 2 also reveals that the boundaries between vesicle-containing and micelle-containing regions of the diagram do not differ substantially on the SDS-rich side when solutions equilibrated for 1 day or 6 months are used. This result contrasts to the behaviors reported for other systems such as CTAB/SOS where the size of the vesicle lobe shrinks during equilibration.[29] The vesicle region on the SDS-rich side of the diagram appears to extend close to the equimolar line; solutions containing 30 mol % BTHA are stable for months against precipitation, whereas samples containing 33 mol % BTHA precipitate within 1 day of preparation. Bonini et al. have also reported on the microstructures formed in several SDS-rich solutions containing SDS and BTHA (after one night of equilibration).[16] The compositions investigated by Bonini et al. are indicated with solid squares in Figure 2A. The microstructures identified in their study are consistent with our measurements and the boundaries drawn between microstructures in Figure 2.

Following visual inspection, we performed QLS measurements to determine the hydrodynamic diameters of any aggregates present in solution. As an example of the data obtained by QLS, results for a series of solutions containing 0.5 wt % total surfactant after 1 day of equilibration at 25 °C are presented in Table 1. Inspection of Table 1 reveals that solutions with 10 mol % BTHA or less have small hydrodynamic diameters. The average diameter of the aggregates is ∼15 nm, which suggests the presence of small rods or elongated micelles. In contrast, samples containing 20 mol % BTHA or more have hydrodynamic diameters of 120 nm or larger, consistent with the presence of vesicles. In all cases, the hydrodynamic diameter reported in H_2O differs only slightly from that in D_2O, indicating that substitution of D_2O for H_2O (as needed for SANS, reported below) has a minimal effect on the aggregate sizes on the SDS-rich side of the composition diagram.[30,41,42] The hydrodynamic sizes of samples containing micelles (as indicated in Figure 2) at concentrations other than 0.5 wt % total surfactant were similar to those reported in Table 1. For samples containing vesicles, the hydrodynamic sizes varied as a function of total surfactant concentration. In general, we observed the sizes of the vesicles to decrease with increasing surfactant concentration.

Samples for SANS measurements were prepared in D_2O and equilibrated for 1 day at 25 °C prior to measurement. Results obtained for SDS-rich samples containing 0.5 wt % total surfactant are presented in Figure 3A. Inspection of Figure 3A reveals that samples composed of 5 and 10 mol % BTHA display a maximum at intermediate values of q and a zero slope at low values of q. This result is consistent with the presence of small micelles. The maximum in the data indicates that the micelles repel each other, likely a result of electrostatic interactions. Samples containing 20 and 25 mol % BTHA display different behavior. In general, the data follows a −2 slope, which suggests a bilayer geometry according to Guinier analysis. Slight minima are also observed for both samples at a q value of ∼0.013 Å. The calculated SANS spectrum for a population of monodisperse vesicles does possess minima, but in practice the minima are often smeared out due to polydispersity in the sizes of the vesicles as well as instrumental smearing effects.[43]

The fits to the SANS data presented in Figure 3A are drawn as solid lines. The 5 and 10 mol % BTHA samples were fit best with an ellipsoidal form factor coupled with a structure factor, whereas the 20 and 25 mol % samples were fit best using a polydisperse core−shell model without a structure factor. Inclusion of a structure factor was necessary for the 5 and 10 mol % samples in order to capture the decrease in scattered intensity observed at low q values, whereas the 20 and 25 mol % samples were fit adequately without a structure factor. We examined both a prolate and an oblate ellipsoid model for the micelles. Both models yielded good fits to the data, with nearly identical reduced χ^2 values. Qualitatively, the prolate model fit was slightly better at high q ($q > 0.2$ Å) and thus that is what we report here.

The parameter estimates obtained from the fits to the SANS data are shown in Table 1. Inspection of Table 1 reveals that the 5 and 10 mol % BTHA samples contain micelles that are only slightly elongated; we obtain minor axis lengths of 1.8 and 1.9 nm and major axis lengths of 2.7 and 3.2 nm from our fits. In previous investigations of the aggregation of SDS (either alone or with added hydrotropes), the length of the minor axis was held fixed at 1.7 nm during modeling, and only the major axis was fit.[35,40] This restriction was deemed necessary to avoid parameter estimates that were unphysical, specifically, a minor axis value that was greater than the end-to-end length of the alkyl chain of SDS. We note that the values obtained here are only slightly longer than 1.7 nm and, furthermore, that the presence of BTHA in the aggregate allows the minor axis to be greater than 1.7 nm. Another previous investigation of SDS micelles using SANS revealed that the micelles typically carry a negative charge equal to ∼32 electronic charges.[35] From Table 1, we observe that as BTHA is added to SDS micelles, the charge on the micelles decrease, from 23 electronic charges to 20 as the mole fraction of BTHA is increased from 5 to 10 mol %. Thus, our observation of decreased surface charge coupled with a slight growth in size upon addition of BTHA parallels the growth in

(41) Chang, N. J.; Kaler, E. W. *J. Phys. Chem.* **1985**, *89*, 2996.
(42) Kaler, E. W.; Herrington, K. L.; Murthy, K.; Zasadzinski, J. A. N. *J. Phys. Chem.* **1992**, *96*, 6698−6707.
(43) Pencer, J.; Hallet, F. R. *Phys. Rev. E* **2000**, *61*, 3003−3008.

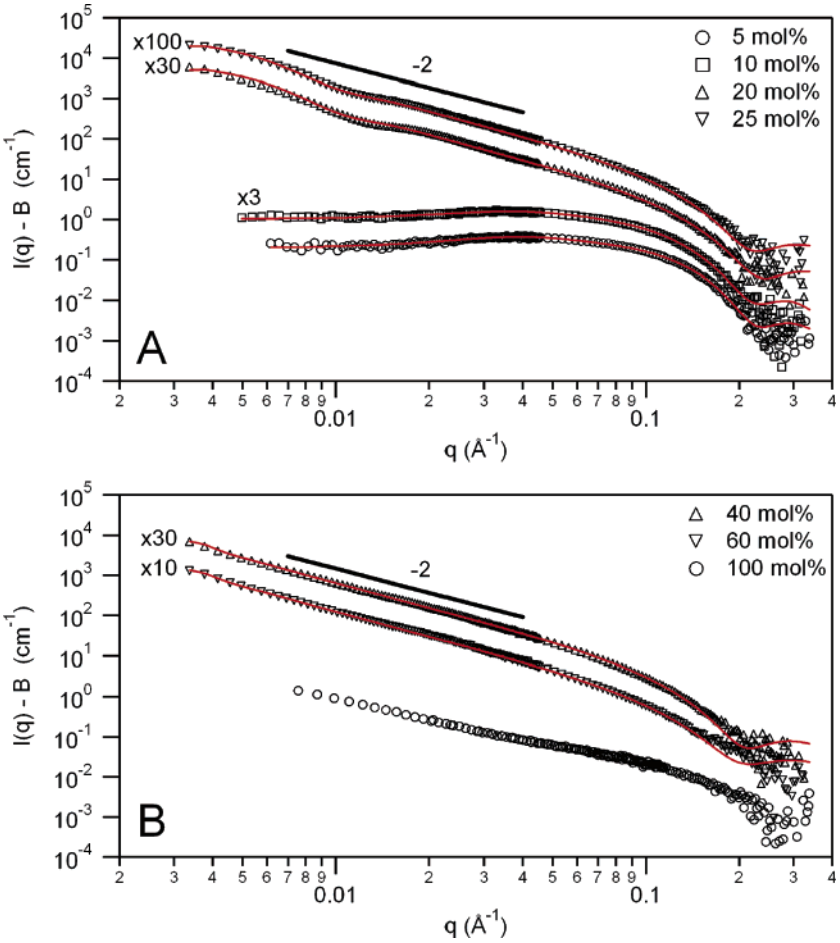

Figure 3. SANS data for a series of BTHA/SDS mixtures containing 0.5 wt % total surfactant. SDS-rich samples are shown in (A), and BTHA-rich samples are shown in (B). The markers represent the data, and the solid lines represent fits to the data using an appropriate form factor model. The data have been offset by the indicated factors for clarity.

micelle size and reduction in surface charge due to addition of cationic hydrotropes observed in other work.[35]

The quality of the polydisperse core−shell model fits to the 20 and 25 mol % BTHA samples supports our conclusion that small vesicles are present in these solutions (see Figure 3A). The vesicles are ∼50 nm in diameter, with bilayer thicknesses of 2.6−2.8 nm (Table 1). These results are in agreement with our previous work,[5] where we reported that a solution composed of 0.1 wt % total surfactant and 15 mol % BTHA/85 mol % SDS contained vesicles 66 nm in diameter on average, with bilayer thicknesses of 2.8 nm (according to the form factor fit). For surfactant aggregates, it is generally accepted that H_2O penetrates into the head group region, up to 1−2 carbons deep into the hydrocarbon layer,[30] thus reducing the apparent thickness measured by SANS. If we calculate the length of the BTHA molecule without including the trimethylammonium head groups, we obtain a value of 2.8 nm, which is in excellent agreement with the results obtained from the form factor fits (Table 1) as well as past results by us and other.[165] When combined, all these results provide further evidence that BTHA likely spans the bilayer of vesicles formed in solution.[5]

Finally, we note that, for all SDS-rich samples listed in Table 1, the aggregate sizes obtained from QLS measurements are larger than those obtained from SANS measurements. Several factors likely cause this difference in the apparent size. First, for samples that contain micelles, our analysis of the QLS data does not consider the effects of repulsive micelle−micelle interactions that may cause the apparent size of the aggregates to be larger than the physical size. Second, and probably more importantly, for polydisperse samples, the QLS-based size estimates will be strongly biased toward the larger aggregates in solution.[5,36,44] Analysis of the QLS data yields the ratio of the fourth to third moment of the number average size distribution,[45] whereas SANS reflects the true number average distribution. Thus, a small number of large objects can substantially distort the average diameter reported by QLS.

BTHA-Rich Solutions. Visual inspection of solutions containing 100 mol % BTHA revealed the solutions to be transparent, similar in appearance to SDS-rich solutions containing micelles. Solutions containing BTHA-rich mixtures of SDS and BTHA, however, were all slightly turbid and resembled SDS-rich solutions that contained vesicles. As summarized in Figure 2A, the QLS and SANS results lead us to conclude that addition of SDS to BTHA results in formation of vesicles after 1 day of equilibration (BTHA-rich solutions). Following equilibration for 6 months, however, the range of compositions that form vesicles on the BTHA-rich side of the diagram shrinks considerably in favor of a two-phase system containing vesicles and precipitate. This observation is similar to solutions containing CTAB and SOS, where the vesicle lobe shrinks during equilibration in favor of a two phase region containing vesicles and lamellae.[29]

Quasi-elastic light scattering results for several BTHA-rich samples containing 0.5 wt % total surfactant are presented in Table 1. Inspection of Table 1 reveals that solutions composed of 40 or 60 mol % BTHA contain aggregates with hydrodynamic

(44) Liu, S.; Gonzalez, Y. I.; Kaler, E. W. *Langmuir* **2003**, *19*, 10732−10738.
(45) Coldren, B.; van Zanten, R.; Mackel, M. J.; Zasadzinski, J. A.; Jung, H. T. *Langmuir* **2003**, *19*, 5632−5639.

sizes that are larger than those observed for vesicles on the SDS-rich side of the diagram. Our QLS results for the 100 mol % BTHA sample also indicate that aggregates with hydrodynamic sizes of ~80 nm are present in solution. This size is too large to correspond to globular micelles and suggests that other structures may be present in solution. Bonini et al. studied a 1 mM (0.07 wt %) BTHA solution using cryo-TEM and reported a mixture of micelles, disks, as well as "closed hollow structures" formed in solution.[16] Although cryo-TEM involves significant shearing of the sample that can cause changes in microstructure,[46] their results suggest that BTHA does not form solutions composed predominantly of globular aggregates. The aggregate size that we measured by QLS is consistent with the presence of disks or vesicles in solution.

The SANS spectra for a series of BTHA-rich samples is shown in Figure 3B. For the 40 and 60 mol % BTHA samples, the data follow a −2 slope, indicative of bilayer geometry according to Guinier analysis. In contrast to the SDS-rich samples that contained vesicles, no minimums are evident in the data. This result could be due to increased polydispersity of the aggregates or simply reflect the fact that the aggregates in solution are larger on the BTHA-rich side than on the SDS-rich side of the microstructure diagram. In the latter case, minima could be present at low q values that lie outside the range of the NG3 instrument. We used the polydisperse core−shell model described above to fit the SANS data from the 40 and 60 mol % BTHA samples. Qualitatively the fits are good, and the parameter estimates obtained are shown in Table 1. Because distinct minima are not observed in the SANS data from the 40 and 60 mol % samples, the QLS measurements also presented in Table 1 provide a more reliable estimate of the sizes of the vesicles in these samples. Inspection of Table 1 reveals that the bilayer thicknesses are ~2.9 nm on the BTHA-rich side of the microstructure diagram. Thus, the bilayer thicknesses change negligibly as a function of the mixing ratio of BTHA to SDS in bulk solution. This result again suggests that BTHA spans the bilayer of vesicles formed in solution, thus constraining the thickness of the bilayer to the end-to-end thickness of the BTHA molecule.

The SANS spectrum for a 0.5 wt % sample of BTHA only is also shown in Figure 3B. We attempted to fit these data using several different form factor models including ellipsoids, rods, and vesicles, each with and without a structure factor, but were unable to obtain a satisfactory fit. Qualitatively, the slope of the data is less than −2 at low q values, which suggests that more than one type of aggregate structure may be present in solution (consistent with the findings of Bonini et al., as discussed above).[16] Both disks and vesicles exhibit a slope of −2 at low q values, whereas micelles display a zero slope at low q values. The presence of disks, vesicles, or both in solution is also supported by our QLS results, as we determined that aggregate microstructures with hydrodynamic diameters of ~80 nm were present in solution.

2. Characterization of the Photostationary State in Aqueous Mixtures of BTHA and SDS. Bonini et al. reported that the compositions of the photostationary states of their aqueous mixtures of BTHA and SDS were dependent on the mixing ratio of BTHA and SDS in solution.[16] The extent of isomerization of the *trans*-BTHA in solution was reported to range from 50 to 75%, depending on mixing ratio of BTHA to SDS. Because the extent of isomerization of BTHA in solution will likely affect the types of microstructure that form in solution following photoisomerization of the BTHA, and because the light source used to drive the photoisomerization will affect the composition

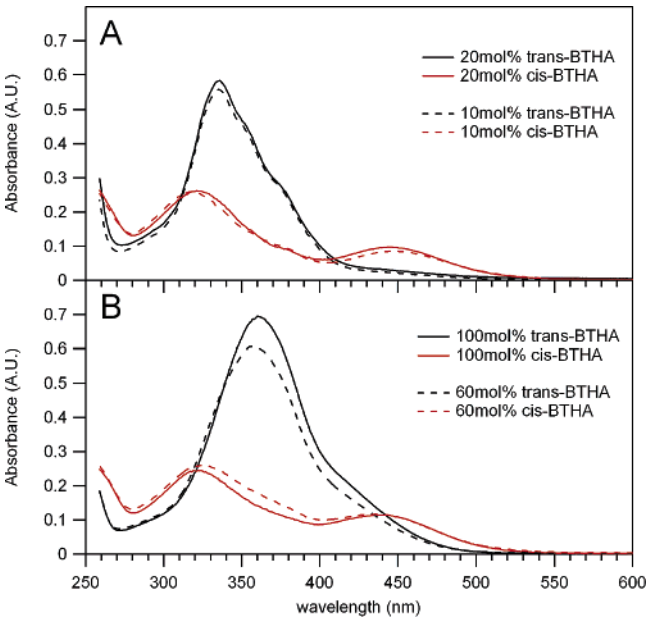

Figure 4. UV−vis spectra: (A) SDS-rich, (B) BTHA-rich. Black lines correspond to mixtures of *trans*-BTHA and SDS, and red lines correspond to mixtures of BTHA and SDS enriched in cis isomer of BTHA by illumination with UV light.

of the photostationary state, prior to determining the microstructures formed in cis-rich BTHA solutions of BTHA and SDS, we sought to determine the extent of isomerization of BTHA in our experimental system by using UV−vis measurements.

We emphasize here that we used UV−vis measurements to determine the extent of isomerization of BTHA in solution. We did not attempt to use UV−vis measurements to characterize the microenvironment of BTHA present in mixtures with SDS. As described in the Methods section, because the molar absorptivity of BTHA is high, it was necessary to dilute all solutions to 30 μM BTHA prior to measurement of the UV−vis spectra. Although the microenvironment of the BTHA is expected to change upon dilution, the extent of isomerization of the BTHA is not expected to change. Figure 4 shows the UV−vis spectra of diluted solutions that contained 0.5 wt % total surfactant and 10, 20, 60, or 100 mol % BTHA prior to dilution. The black lines in Figure 4 represent the UV−vis spectra of a solution containing *trans*-BTHA and SDS. Red lines represent the UV−vis spectra of solutions that were isomerized to the photostationary state with UV light, diluted to 30 μM BTHA, and then measured. Examination of Figure 4B reveals that solutions containing 100 mol % *trans*-BTHA exhibit a single absorption peak at 360 nm. The peak is symmetric, tailing slightly for λ > 400 nm. The spectrum for the 60 mol % BTHA sample closely resembles that of a 100 mol % BTHA sample, except that the peak absorbance has decreased and has shifted slightly to 357 nm. As seen in Figure 4A, the spectra obtained from samples that are SDS-rich are qualitatively different from those that are BTHA-rich. The peak absorbances are lower than the BTHA-rich samples and have shifted to 335 nm. Two shoulder peaks are evident in the spectra, and the tailing behavior observed at λ > 400 nm for the 100 mol % *trans*-BTHA sample is suppressed.

Inspection of Figure 4 reveals that the photostationary state obtained in our experiments does not depend strongly on the mixing ratio of BTHA to SDS, as evidenced by the fact that the peak absorbances for the cis samples are nearly identical for the 10, 20, 60, and 100 mol % BTHA samples. From these UV−vis spectra, we calculated that solutions enriched in the cis isomer of BTHA contained 75−80% cis isomers, independent of

(46) Danino, D.; Weihs, D.; Zana, R.; Orädd, G.; Lindblom, G.; Abe, M.; Talmon, Y. *J. Colloid Interface Sci.* **2003**, *259*, 382−390.

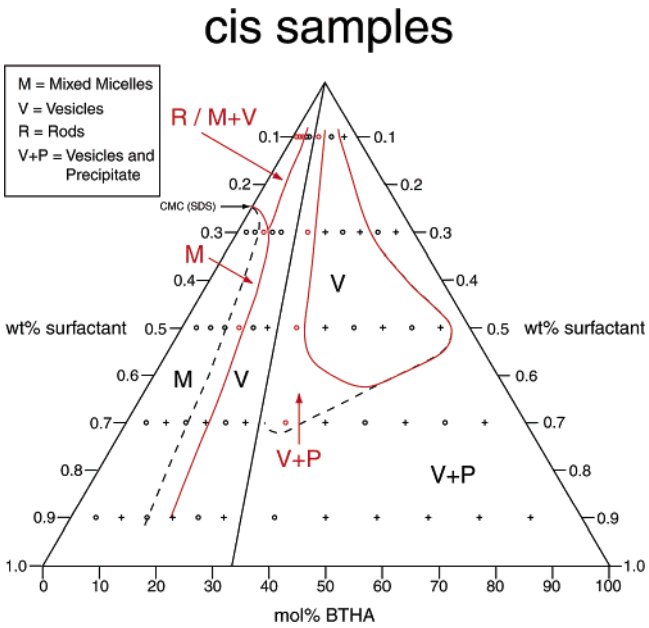

Figure 5. Microstructure diagram for SDS/*cis*-BTHA/H_2O. Dashed lines represent the boundaries from the 6-month diagram, and the solid lines indicate the new boundaries formed after isomerization. Samples that undergo a change in the type of microstructure upon isomerization are marked in red.

composition. In contrast, and mentioned above, Bonini et al. reported that their samples containing a fixed concentration of BTHA and different concentrations of SDS contained as little as 50% or as much as 75% of the cis isomer of BTHA after illumination with UV light. Bonini et al. also reported that, after illumination of a solution rich in the cis isomer of BTHA with light at 430 nm, as little as 55% or as much as 85% of the BTHA was converted back to the trans state, the amount depending on the mixing ratio of BTHA and SDS.[16] However, for all compositions that we investigated, illumination with an incandescent bulb resulted in solutions that contained at least 90% *trans*-BTHA. A representative example of this behavior can be found in Supporting Information.

We believe that our conclusions regarding the compositions of the photostationary states differ from those reported by Bonini et al. because the light sources used in the two studies are different. Bonini et al. used monochromatic UV (365 nm) and visible (430 nm) light sources.[16] In contrast, in the study reported here, we used broadband light sources for both UV and visible illumination. The photostationary state that is achieved upon illumination with a broadband light source depends on the ratio of absorbance of the trans and cis isomer at each wavelength, the photoefficiency of the trans-to-cis isomerization at each wavelength, and the relative intensity of each wavelength in the spread.[47] Our decision to use a broadband light source was motivated by the observation that the peak absorbance shifts from 360 nm when BTHA is alone in solution (Figure 4B) to 335 nm when mixed with SDS (Figure 4A). Similarly, the ratio of absorbance of the trans and cis isomers for wavelengths between 400 and 500 nm changes markedly between solutions that contain BTHA only (Figure 4B) or BTHA and SDS (Figure 4). The broadband light sources used in our study have the advantage that they yield photostationary states that are relatively insensitive to composition of BTHA and SDS in solution.

3. Phase Behavior and Microstructure of Solutions Rich in *cis*-BTHA and SDS. Figure 5 shows microstructures that we determined to form in solution following illumination of mixtures of BTHA and SDS with UV light. As discussed above, 75−80% of the BTHA in these solutions is present as the cis isomer. The boundaries between microstructures present in solution after isomerization of BTHA to the photostationary state are shown as solid red lines. For comparison, the boundaries between microstructures for mixtures of *trans*-BTHA and SDS (as reported in Figure 2B) are shown as dashed lines. The regions between the dashed and solid lines thus indicate regions of composition where pronounced changes in microstructure occur upon isomerization. These regions are marked with arrows, and samples within these regions that were characterized in detail (by QLS and SANS, see below) are marked with red circles. Here we note that all the UV-induced transformations in microstructure observed on the SDS-rich side of the composition diagram were found to be completely reversible: the transformation could be reversed by illumination with visible light or by equilibration of the solutions overnight in the dark. Some of the transformations on the BTHA-rich side of the composition diagram (as discussed below) were not reversible. We have organized our presentation of QLS and SANS results below by dividing the composition diagram into four regions.

Region 1: ≥0.3 wt % Total Surfactant, 15−20 mol % BTHA. The SANS spectra of samples representative of region 1 (0.3 wt % total surfactant, 15 mol % BTHA/85 mol % SDS) are shown in Figure 6. Samples of this composition were treated as follows. First, a solution containing *trans*-BTHA and SDS was prepared and equilibrated in the dark for 1 week prior to measurement. The SANS spectrum for this sample is plotted with open circles. A second sample was illuminated with UV light until the photostationary state was reached, inserted into the SANS instrument, and scattering was recorded while the sample was continuously illuminated with UV light. The spectrum thus obtained is plotted as open triangles in Figure 6. A third sample was illuminated with UV light until the photostationary state was reached and subsequently illuminated with visible light. This sample was then equilibrated in the dark for 1 week prior to running a SANS measurement. Designated as TCT (trans to cis to trans), the spectrum recorded for this sample is plotted as open squares in Figure 6. The data sets in Figure 6 have been offset by the indicated factors for clarity.

Inspection of Figure 6 reveals that the trans and the TCT samples both follow a −2 slope, indicative of a bilayer geometry according to Guinier analysis. These samples were thus fit with the polydisperse core−shell model, and the fits obtained are plotted as red lines through the data. Qualitatively, the fits to the data are excellent, and the parameter estimates generated are shown in Table 2. Form factor fits to the SANS data (as well as QLS measurements) reveal that the vesicle diameters for the trans (78 nm) and TCT (70 nm) samples are nearly identical, although vesicles in the TCT sample are more polydisperse. Because of the absence of a minimum in the SANS data of the TCT sample, we place greater reliance on the sizes of the vesicles in the TCT sample that were obtained by using the QLS measurements. The bilayer thicknesses calculated for both samples are also in excellent agreement (2.8 vs 2.7 nm).

Examination of the SANS spectrum for the cis-rich sample in Figure 6 reveals that the aggregates in solution are markedly different from those for the trans and TCT samples. The data display a distinct maximum, followed by a zero slope at low q values, consistent with the presence of small, globular micelles. The data were fit using an ellipsoidal form factor coupled with the structure factor described above. Again, both a prolate and an oblate ellipsoidal form factor were tested, and in this case,

(47) Meier, H. *Angew. Chem., Int. Ed. Engl.* **1992**, *31*, 1399−1420.

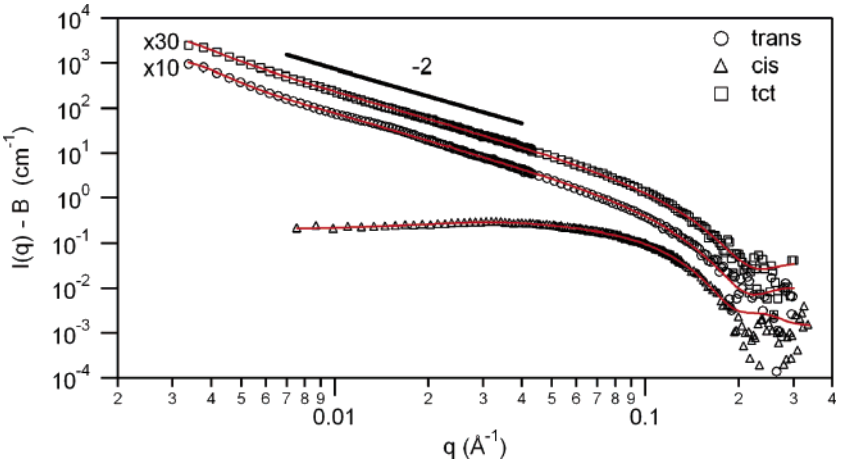

Figure 6. SANS data for solutions containing 0.3 wt % total surfactant and 15 mol % BTHA/85 mol % SDS, before and after isomerization with UV light, and after isomerization with UV and then visible light. The markers represent the data, and the solid lines represent fits to the data using an appropriate form factor model. The data have been offset by the indicated factors for clarity.

Table 2. Quasi-Elastic Light Scattering Results and Parameter Estimates Obtained from Form Factor Fits to the SANS Data for the Solutions Containing 0.3 wt % Total Surfactant and 15 mol % BTHA/85 mol % SDS Presented in Figure 6

sample	QLS intensity (kcounts/s) H_2O/D_2O	QLS diameter (nm) H_2O/D_2O	form factor diam (nm)	polydis-persity	bilayer thickness (nm)	$\sqrt{\chi^2/N}$
trans	155/168	162/198	78	.54	2.8	3.0
TCT	122/133	131/149	70	.73	2.7	2.1

sample	QLS intensity (kcounts/s) H_2O/D_2O	QLS diameter (nm) H_2O/D_2O	major axis (nm)	minor axis (nm)	charge (e)	$\sqrt{\chi^2/N}$
cis	12/12	102/119	2.7	1.7	23	1.3

the oblate model yielded a slightly better reduced χ^2 value (the latter model is reported here). From Table 2, we observe that the major axis of the micelles is 2.7 nm. We calculate a micelle charge of 23 from the structure factor. Comparing this result to the sample containing 0.5 wt % surfactant and 5 mol % *trans*-BTHA/95 mol % SDS (see Table 1), we observe that the sizes of the micelles are identical, according to the form factor fit. Thus, although the cis sample contains a higher fraction of BTHA (15 vs 5 mol %), the micelle charge remains unchanged. This result likely indicates that *cis*-BTHA is not incorporated into the micelles to the same extent as *trans*-BTHA, which may reflect the fact that the cis isomers of azobenzene-containing compounds are less hydrophobic than their trans counterparts.[48]

Although the SANS spectrum for the cis sample (0.3 wt % surfactant, 15 mol % BTHA/85 mol % SDS) clearly reflects the presence of small micelles, we obtained an average diameter of ~100 nm from QLS measurements. The intensity of light scattered from the cis sample, however, is 1 order of magnitude lower than from the trans and TCT samples, indicating that most (roughly 90%) of the vesicles in a solution rich in *cis*-BTHA are disrupted into smaller structures upon isomerization. It is interesting to note that the sizes of the remaining large aggregates reported by QLS following isomerization are similar to the sizes of the vesicles present in solution prior to isomerization with UV light. Because 25% of the BTHA in solution is not converted to the cis isomer upon illumination with UV light, it appears possible that the large aggregates in solution after photoisomerization are vesicles that are composed of the *trans*-BTHA remaining in solution and SDS. This physical picture suggests that there may be segregation of *cis*-BTHA and *trans*-BTHA between the microstructures present at the photostationary state, a proposition that is consistent with additional measurements reported below.

Region 2: <0.3 wt % Surfactant, 5−15 mol % BTHA. In this second region of the microstructure diagram, we observed that UV illumination of solutions resulted in SANS spectra with a slope of −2 prior to illumination and SANS spectra with a slope of −1 after illumination with UV light. In the interests of brevity, we refer the reader to a previous publication in which we reported the SANS spectra (before and after illumination) of solutions containing 0.1 wt % total surfactant, 15 mol % BTHA/85 mol % SDS.[5] The slope of −2 is consistent with the presence of bilayers, according to Guinier analysis, whereas a slope of −1 is consistent with the presence of rodlike aggregates in solution.[33] Bonini et al. have also reported characterization of a solution within region 2, a solution containing 0.2 wt % total surfactant, 17 mol % BTHA/83 mol % SDS. The authors interpreted their QLS and SANS measurements for solutions containing *trans*-BTHA or *cis*-BTHA in terms of a model for a mixture of micelles and vesicles, rather than rodlike micelles. Whether or not the cis-rich solutions that we characterized in this region of the microstructure diagram contain rodlike micelles or mixtures of globular micelles and vesicles cannot be unambiguously determined based on our SANS measurements. We note that because the photostationary state obtained by Bonini et al. is different from our studies (see above), it is also possible that different microstructures are present in the two sets of solutions following illumination. Although there is some uncertainty regarding the microstructure resulting from the illumination of these solutions with UV light, it is apparent that the microstructure or mixture of microstructures present in region 2 differs from region 1. We have marked region 2 in the composition versus microstructure diagram with the symbols R/M+V to indicate that rodlike micelles or a combination of micelles and vesicles may be present in solution after illumination with UV light.

Region 3: 0.1−1.0 wt %, 40 mol % BTHA. Region 3 corresponds to a region of the microstructure diagram that is rich in BTHA. We observed that samples containing 40 mol % BTHA

(48) Yang, L.; Takisawa, N.; Hayashita, T.; Shirahama, K. *J. Phys. Chem.* **1995**, *99*, 8799−8803.

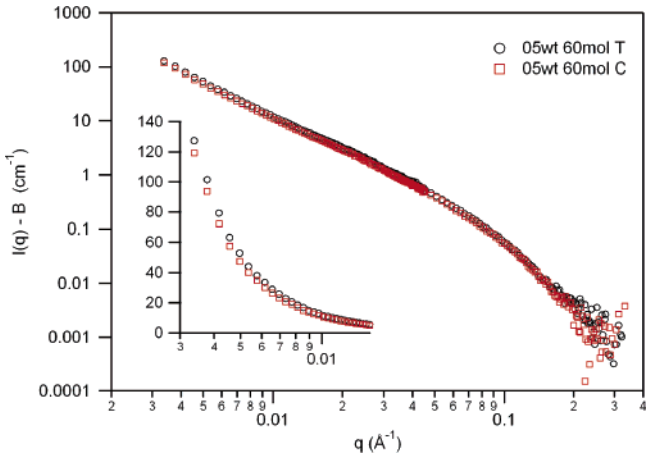

Figure 7. SANS data for solutions containing 0.5 wt % total surfactant and 60 mol % BTHA/40 mol % SDS before (open circles) and after (open squares) isomerization with UV light. Inset: Low *q* region of the SANS data, shown on a linear scale for clarity.

precipitated upon illumination with UV light throughout the range of total surfactant concentrations studied. According to UV−vis measurements, less than 4% of the BTHA remained in solution after illumination with UV light. In contrast to the transformations observed on the SDS-rich side of the microstructure diagram, the precipitation of surfactant induced by UV illumination could not be reversed by illumination with visible light or equilibration at 25 °C in the dark. This result indicates either that the vesicles formed in solution prior to illumination with UV light were not equilibrium structures or that a significant kinetic barrier exists toward reformation of vesicles. Vesicles formed from mixtures containing 40 mol % *trans*-BTHA are stable for 6+ months, whereas other BTHA-rich samples that precipitate do so in less than 1 month. We remark here that the ability to precipitate surfactant from a solution using light could be useful in systems that require the removal of surfactant prior to further processing or analysis.

Region 4: Remainder of Microstrcture Diagram. The results presented above address solution compositions that displayed large changes in phase behavior or aggregate microstructure upon illumination with UV light. Surprisingly, for compositions outside of these regions, illumination of BTHA and SDS solutions with UV light had a relatively minor impact on the phase behavior and microstructure in solution. For such solutions, we observed only minor changes in the SANS spectra and QLS measurements. A representative example is shown in Figure 7 (0.5 wt % total surfactant, 60 mol % BTHA/40 mol % SDS). When plotted on a log scale (similar plot to Figure 3), it appears that there is almost no change in the SANS spectrum upon illumination with UV light. Careful examination of the data on a linear scale reveals that the scattered intensity does decrease by ∼10% after illumination of the solution with UV light. Our QLS measurements of the same solution revealed that the intensity of scattered light decreased from 72.4 to 52.0 kcounts/s after illumination with UV light (a 28% decrease). The apparent hydrodynamic diameter was measured to increase slightly from 256 to 289 nm (the solution for QLS was prepared in D_2O), an effect that likely reflects some change in the distribution of sizes of aggregates in solution. We sought to determine if this modest level of reorganization of the solution was due to the absence of substantial photoisomerization of the BTHA within these mixtures with SDS. We confirmed, however, that the photostationary state formed in solution contained ∼75% *cis*-BTHA.

The above-described observations are interesting in light of our previously mentioned proposition that the trans and cis isomers of BTHA may not be well mixed between microstructures present in the photostationary state. If the aggregates (vesicles) formed in a solution containing 60% BTHA and 40% SDS (molar compositions in bulk solution) are assumed to be electrically neutral, then two-thirds of the BTHA in the solution will be in a state of aggregation that does not involve SDS. Thus, a photostationary state containing 75% *cis*-BTHA could be reached with minimal perturbation of aggregates involving BTHA and SDS (the vesicles in solution). Such a segregation of *trans*- and *cis*-BTHA in solution following isomerization is consistent with several observations reported in this paper. We also note that, in past studies of BTHA and SDS in water, Bonini et al. interpreted UV−vis measurements in terms of segregation of *cis*-BTHA and *trans*-BTHA between micelles and bilayers coexisting in solution.[16] These observations, when combined, suggest that understanding the extent to which the properties of aqueous solutions containing BTHA and SDS can be tuned by light will require, in general, consideration of the possible segregation of *cis*-BTHA and *trans*-BTHA species between microstructures in solution. Here we also note that if segregation of trans and cis isomers of BTHA between coexisting microstructures turns out to be a general behavior of this system, knowledge of the composition of the photostationary state (fraction of BTHA present in cis state) may provide a relatively simple means to predict (approximately) the relative abundance of coexisting microstructures in solution.

Conclusions

The study reported in this paper characterizes the microstructures formed by aqueous mixtures containing SDS and BTHA, with total surfactant concentrations less than 1% by weight, before and after illumination with UV light. Prior to illumination with UV light, microstructures such as mixed micelles and vesicles are observed in solutions containing *trans*-BTHA and SDS. Similar to the CTAB/SOS system, for example, mixed micelles form in solutions that contain a concentration of the anionic surfactant above its cmc, and precipitation is observed for all samples that contain an equal number of oppositely charged surfactant head groups. In contrast to surfactant systems such as CTAB/SOS, the width of the vesicle lobe (after 6 months of equilibration) appears to be greater for solutions that are rich in BTHA. We also characterized the composition of the photostationary state of UV-illuminated solutions and determined these solutions to contain 75−80% *cis*-BTHA, independent of the mixing ratio of SDS and BTHA in solution. Illumination of a *cis*-BTHA-rich solution with visible light resulted in a solution with 90+% trans isomers. Although the composition of the photostationary state (% *cis*-BTHA) was determined to be largely invariant throughout the microstructure diagram, substantial changes in microstructure upon illumination with UV light were observed for a limited range of compositions only. On the SDS-rich side of the microstructure diagram, vesicles were observed to be transformed into globular or rodlike micelles. On the BTHA-rich side of the microstructure diagram, the most dramatic change in microstructure was accompanied by precipitation. Elsewhere in the microstructure diagram, illumination of solutions with UV light resulted in modest changes in microstructure, which in some regions of the microstructure diagram may be due to a segregation of *cis*-BTHA and *trans*-BTHA isomers between aggregate microstructures coexisting in solution.

Acknowledgment. We acknowledge the support of the National Institute of Standards and Technology, U.S. Department

of Commerce, in providing the neutron facilities used in this work. This work utilized facilities supported in part by the National Science Foundation under agreement DMR-9986442, CTS-0327489, CTS-0553760, and DMR-0602570. Financial support from the donors to the Petroleum Research Fund (44193-AC7) is also acknowledged.

Supporting Information Available: Additional information given in text. This material is available free of charge via the Internet at http://pubs.acs.org.

LA0632124